

Concentration quenching in fine-grained ceramic Nd:YAG

Larry D. Merkle and Mark Dubinskii

Army Research Laboratory, AMSRD-ARL-SE-EO
2800 Powder Mill Rd, Adelphi, MD 20783
lmerkle@arl.army.mil

Kenneth L. Schepler and S. M. Hegde*

Air Force Research Laboratory, AFRL/SNJW
2241 Avionics Circle, Wright-Patterson AFB OH 45433-7304

*Also at the University of Dayton Research Institute, Dayton, OH 45469-0175

Abstract: We have studied the concentration dependent fluorescence decay kinetics of ceramic Nd:YAG, to resolve inconsistencies in the previous literature. Our data indicate that earlier reports of single exponential lifetimes even at Nd concentrations of a few percent were due to the effects of long-pulse excitation. Under short-pulse excitation the fluorescence decay is nonexponential for concentrations greater than about 1% atomic. Energy migration to sinks consisting of cross-relaxing Nd ions dominates at long times, whereas single-step energy transfer to randomly distributed quenching sites dominates at earlier times. The concentration dependence of this single-step transfer indicates direct cross-relaxation between individual ions at concentrations below 4% atomic, but resonant transfer to quenching sites consisting of Nd pairs at higher concentrations.

©2006 Optical Society of America

OCIS codes: (140.3380) Laser materials; (160.5690) Rare earth doped materials

References and links

1. J. Lu, K. Ueda, H. Yagi, T. Yanagitani, Y. Akiyama and A. A. Kaminskii, "Neodymium doped yttrium aluminum garnet ($Y_3Al_5O_{12}$) nanocrystalline ceramics—a new generation of solid state laser and optical materials," *J. Alloys Compd.* **341**, 220-225 (2002).
2. V. Lupei, A. Lupei, S. Georgescu, B. Diaconescu, T. Taira, Y. Sato, S. Kurimura and A. Ikesue, "High-resolution spectroscopy and emission decay in concentrated Nd:YAG ceramics," *J. Opt. Soc. Am. B* **19**, 360-368 (2002).
3. R. C. Powell, *Physics of Solid-State Laser Materials*, (AIP Press, New York, 1998), p. 334.
4. V. Lupei, T. Taira, A. Lupei, N. Pavel, I. Shoji and A. Ikesue, "Spectroscopy and laser emission under hot band resonant pump in highly doped Nd:YAG ceramics," *Opt. Commun.* **195**, 225-232 (2001).
5. G. A. Kumar, J. Lu, A. A. Kaminskii, K. Ueda, H. Yagi, T. Yanagitani and N. V. Unnikrishnan, "Spectroscopic and stimulated emission characteristics of Nd^{3+} in transparent YAG ceramics," *IEEE J. Quantum Electron.* **40**, 747-758 (2004).
6. V. Lupei and A. Lupei, "Emission dynamics of the $^4F_{3/2}$ level of Nd^{3+} in YAG at low pump intensities," *Phys. Rev. B* **61**, 8087-8098 (2000).
7. L. A. Diaz-Torres, O. Barbosa-Garcia, J. M. Hernandez, V. Pinto-Robledo and D. Sumida, "Evidence of energy transfer among Nd ions in Nd:YAG driven by a mixture of exchange and multipolar interactions," *Opt. Mater.* **10**, 319-326 (1998).
8. M. J. Weber, "Luminescence decay by energy migration and transfer: Observation of diffusion-limited relaxation," *Phys. Rev. B* **4**, 2932-2939 (1971).
9. K. B. Eisenthal and S. Siegel, "Influence of resonance transfer on luminescence decay," *J. Chem. Phys.* **41**, 652-655 (1964). See also references 1-3 therein.
10. M. Yokota and O. Tanimoto, "Effects of diffusion on energy transfer by resonance," *J. Phys. Soc. Jpn.* **22**, 779-784 (1967).
11. A. Lupei, V. Lupei, S. Georgescu, C. Ionescu and W. M. Yen, "Mechanisms of energy transfer between Nd^{3+} ions in YAG," *J. Lumin.* **39**, 35-43 (1987).

12. R. C. Powell, *op cit*, p. 199.
 13. A. Ikesue, T. Kinoshita, K. Kamata and K. Yoshida, "Fabrication and optical properties of high-performance polycrystalline Nd:YAG ceramics for solid-state lasers," *J. Am. Ceram. Soc.* **78**, 1033-1040 (1995).
 14. H. G. Danielmeyer, M. Blatte and P. Balmer, "Fluorescence quenching in Nd:YAG," *Appl. Phys.* **1**, 269-274 (1973).
 15. R. C. Powell, *op cit*, p. 325.
 16. M. Dubinskii, L. D. Merkle, J. R. Goff, V. K. Castillo and G. J. Quarles, "Laser Studies of 8% Nd:YAG Ceramic Gain Material," in *OSA Trends in Optics and Photonics Series (TOPS) Vol. 98, Advanced Solid-State Photonics*, Craig Denman, ed. (Optical Society of America, Washington, DC 2005), pp. 47-51.
-

1. Introduction

Dramatic improvements in transparency in recent years have made ceramic laser materials such as Nd-doped YAG (yttrium aluminum garnet, $Y_3Al_5O_{12}$) very promising competitors for the customary single-crystal laser gain media [1, 2]. In addition to scalability, superior mechanical strength, control over dopant profile and potentially lower production costs, ceramic Nd:YAG is interesting because it can accommodate substantially higher concentrations of neodymium and still retain useful optical quality. However, ceramic technology cannot circumvent the well-known cross-relaxation process that causes substantial concentration quenching in Nd-doped materials, including YAG [3].

Over the concentration range in which single-crystal and ceramic Nd:YAG can be compared, concentration quenching of the Nd^{3+} fluorescence is essentially identical in ceramic and single-crystal samples [1]. Several studies of quenching at higher Nd concentrations in ceramics have been reported, with somewhat inconsistent results. In particular, detailed investigations of the relatively large-grained ceramic Nd:YAG developed at the Japan Fine Ceramics Center showed distinctly nonexponential luminescence decay for concentrations above about 3% atomic under excitation at both 532 nm (into $^4G_{7/2}$) and 885 nm (into $^4F_{3/2}$) [2, 4]. The similarity of decay kinetics for these two excitation wavelengths is not surprising, since it is widely accepted that many closely-spaced excited manifolds in Nd^{3+} , including $^4G_{7/2}$, decay very efficiently and rapidly to the metastable $^4F_{3/2}$ manifold by nonradiative processes. However, Kumar *et al.* recently reported single-exponential decay for concentrations up to at least 4% atomic of the finer-grained ceramic Nd:YAG material from Konoshima Chemicals, when excited at 807 nm [5]. It is important that this difference in decay kinetics be clarified, since laser application of highly concentrated ceramic Nd:YAG requires knowledge of the energy storage time, and since 807 nm is essentially the same as the most commonly used diode pump wavelength for Nd:YAG lasers.

Another uncertainty regarding concentration quenching in Nd:YAG arises from recent studies of relatively low-concentration single-crystal samples. V. Lupei and A. Lupei interpreted this quenching in terms of direct cross-relaxation between excited Nd ions and randomly spaced unexcited ions [6]. Since the concentration of acceptors in this model is essentially equal to the total Nd concentration, they found that relatively small transfer rate parameters were required to fit the data. However, Diaz-Torres *et al.* interpreted quenching in the same system in terms of resonant energy transfer to quenching centers consisting of perturbed Nd ions [7]. Their fitting gave much larger transfer rate parameters and an order of magnitude smaller quenching center concentration for a given Nd concentration. The model of Lupei and Lupei is consistent with a linear dependence of the energy transfer rate on Nd concentration, whereas the concentration dependence to be expected for the model of Diaz-Torres *et al.* depends on the nature of the quenching centers. Thus, high concentration studies hold the potential to clarify the nature of the energy transfer.

We report here the results of concentration quenching studies on Konoshima Nd:YAG ceramic samples with concentrations in the range 0.09% to 9% atomic. We compare results for excitation wavelengths of 532 nm and 808 nm. The results allow us to address the

disagreements noted above, and also highlight complications that arise due to inhomogeneities in highly concentrated samples.

2. Experimental details

All materials studied were fine-grained (1-3 μm typical size) ceramic Nd:YAG from Konoshima Chemicals Company, fabricated into spectroscopic samples by the VLOC subsidiary of II-VI Inc. The nominal Nd concentrations studied were 0.09, 1, 2, 4, 8 and 9% atomic. The 1%, 4% and 9% samples were analyzed by the Alabama A&M University Research Institute using Rutherford backscattering, yielding Nd concentrations of 1.01%, 3.71% and 9.09%, respectively. Since these results are not available for all samples but indicate that the nominal values are reasonably accurate, we used the nominal values in analyses of the quenching data for all samples for consistency.

Fluorescence lifetimes were measured by detecting the ${}^4F_{3/2} \rightarrow {}^4I_{9/2}$ fluorescence near 885 nm using an Instruments SA 0.3-m monochromator, a Hamamatsu photomultiplier tube with S-1-like response and a Tektronix digital oscilloscope. The maximum load resistance was 560 Ω , giving an estimated instrumental time constant of 100 ns or less, and most data were taken using a load resistance of 50 Ω . All data were taken at room temperature.

The excitation source for 532-nm pumping was a Q-switched, frequency-doubled Continuum Nd:YAG laser with about 8 ns pulse duration. A Lambda-Physik optical parametric oscillator pumped by a Q-switched, frequency-tripled Coherent Nd:YAG laser provided 3-ns pulses for 808-nm excitation.

3. Data with excitation at 532 nm

The room temperature fluorescence decay of the 0.09% Nd:YAG sample under 532-nm excitation is exponential, with a lifetime of 262 μs , and that of the 1% Nd sample deviates from a single exponential only subtly. For the higher Nd concentrations the deviation from exponential is much more substantial. This must indicate concentration-dependent quenching, such that the decay can be expressed as

$$n_{\text{excited}}(t) = n_0 \times \exp(-t/\tau_0 - P(t)), \quad (1)$$

where n_0 is the initial concentration of excited ions, τ_0 is the intrinsic lifetime of an isolated Nd ion and $P(t)$ characterizes the time-dependent quenching. $P(t)$ is shown in Fig. 1 for the four higher concentrations, taking τ_0 as 262 μs . In each case the function becomes linear at long times, indicative of an exponential decay.

These curves are fit rather well for all concentrations by a model that combines the square root of time exponent expected for single-step electric-dipole-dipole transfer to randomly spaced quenching centers and a concentration-dependent exponential decay that dominates at long times. Similar to a method used by Weber [8], we fit these decay curves using the mathematical expression of Eisenthal and Siegel with the tail exponential decay rate interpreted as that due to energy migration to quenching centers, rather than to intrinsic intra-ionic decay alone as in their original model [9]. Thus,

$$P(t) = (4/3)\pi^{3/2}n_a(\alpha t)^{1/2} + Wt, \quad (2)$$

where n_a is the concentration of acceptors, α is the rate constant for the single-step, random-distance electric-dipole-dipole energy transfer and W is the quenching rate due to migration to traps. We find that this simple expression provides more stable fits to the data than does the somewhat more complex expression derived for the combination of single-step and migration transfer by Yokota and Tanimoto[10].

As Fig. 1 shows, the fits to the data are quite satisfactory. The poorest fit is that for 2% Nd, for which it is just discernible in the inset of Fig. 1(b) that the fit (the dashed curve) differs from the data. This is due to an initial decay that is less steep than predicted by the

model, consistent with the approximately exponential initial decay reported by others [6, 11]. Those reports attribute this behavior, quite plausibly, to the discrete distribution of acceptor ions, imposing a finite minimum donor-acceptor spacing in contradistinction to the model's uniform acceptor distribution. This results in a slower initial decay than the model predicts. We obtain a much better fit to all but the first several microseconds of the decay by scaling n_0 of Eq. (1) higher by about $\exp(0.05)$ to account for that slower initial decay. Throughout this study, we find that such an initial exponential decay is most likely to be observed at low to moderate concentrations, rather than at 8 or 9% Nd.

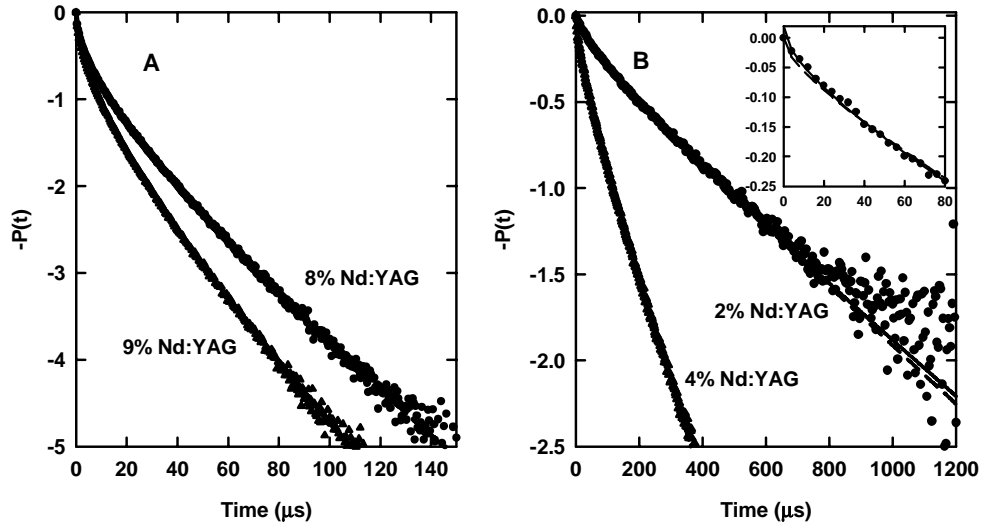


Fig. 1. Quenching function $P(t)$, as defined by Eq. (1) in the text with $\tau_0 = 262 \mu\text{s}$, for the 532-nm excited fluorescence of bulk samples of ceramic Nd:YAG for four concentrations. The inset to B shows early-time details of the decay and fits for 2% Nd. In each case the discrete symbols represent the experimental data. Fits to Eq. (2) are shown as solid and dashed curves. For 2% Nd the fit shown as a solid curve has its amplitude scaled to fit the portion of the decay after the initial approximately exponential decay, whereas the fit shown as a dashed curve is an attempt to fit the entire decay at once.

Data were taken at 532-nm pumping intensities differing by more than an order of magnitude, resulting in no difference in decay dynamics. Thus heating, upconversion and other nonlinear processes do not appear to be important in these data.

Table 1. Energy transfer parameters versus concentration from fitting Eq. (2) to the fluorescence decay data. A_{ss} is an abbreviation for $(4/3)\pi^{3/2}n_a(\alpha)^{1/2}$. W , n_a and α are defined in the text, and $1/\tau_{\text{tail}} = 1/\tau_0 + W$.

Nd Concentration (% atomic)	532nm Excitation, Bulk			532nm Excitation, Powder			808nm Excitation, Bulk		
	τ_{tail} (μs)	W (s^{-1})	A_{ss} ($\text{s}^{-1/2}$)	τ_{tail} (μs)	W (s^{-1})	A_{ss} ($\text{s}^{-1/2}$)	τ_{tail} (μs)	W (s^{-1})	A_{ss} ($\text{s}^{-1/2}$)
0.09	262	0 ^a	0	250	0 ^a	0	262	0 ^a	0
1	249	200	5.5	244	100	14	260	22	20
2	193	1360	17	195	1130	30	218	770	43
4	117	4730	41	122	4200	67	125	4180	61
8	49	16,590	215	55	14,180	250	59	13,130	260
9	40	21,180	260	45	18,220	300	52	15,410	325

^a Zero by assumption.

The parameters for model fits to the data are given in Table 1. For the single-step transfer to randomly-spaced acceptors separate determination of α depends on knowledge of n_a , so only the combination $n_a\alpha^{1/2}$ is given.

4. Fluorescence decay of powders excited at 532 nm

Since absorption from the $^4I_{9/2}$ ground manifold to the $^4F_{3/2}$ manifold of Nd^{3+} overlaps the emission substantially, the possible effect of radiative reabsorption on the observed fluorescence lifetimes (particularly at higher Nd concentrations) must be considered. We ground small samples of Nd:YAG of each concentration with a mortar and pestle, resulting in powders with sizes estimated by microscopy not to exceed 100-200 μm , and with most of the material in far smaller particles. Although this may not be sufficient to make reabsorption in the 8 and 9% samples completely negligible, it does reduce that absorption dramatically compared to the bulk samples of 2-5mm dimensions.

The resulting decay curves are very similar to those observed for bulk samples, as summarized in Table 1. The lifetime in the long-time limit, or tail lifetime, differs somewhat between the powder and bulk samples. However, the difference is typically only several percent. The signal to noise ratio was poorer for emission from the powders due to their relatively weak absorption, resulting in an estimated uncertainty in the tail lifetimes of about 10%. Thus, the observed differences in tail lifetimes between powder and bulk samples is not significant, and radiative reabsorption need not be considered in interpreting the decay kinetics in terms of energy transfer processes.

The nonexponential portion of the decay is somewhat stronger in the powder data than in the bulk sample data, resulting in the somewhat larger single-step transfer parameters shown in the table. The concentration dependences of both the single-step parameter and the energy migration rate are similar for the two types of sample.

5. Data with excitation at 808 nm

As for 532-nm excitation, the fluorescence lifetime of the 0.09% Nd:YAG bulk sample under excitation by 808-nm pulses of 3-ns duration is a single exponential with a lifetime of 262 μs . As the quenching function plots in Fig. 2 indicate, the decays for all higher concentrations for this excitation wavelength are qualitatively similar to those for 532-nm excitation, and in particular are distinctly nonexponential, consistent with Lupei *et al.* [4], but clearly at variance with Kumar *et al.* [5]. However, comparison of Figs. 1 and 2 shows significant quantitative differences. The quenching for a given concentration tends to be somewhat stronger for 808-nm excitation, and the agreement with Eq. (2) is slightly poorer, though still reasonable. For some concentrations, the initial 0.1 or 0.2 e-folding of the decay resembles an exponential more clearly than was true for 532-nm excitation. This is particularly evident for the 2% Nd sample's decay. As shown in Fig. 2(B), straightforward fitting with Eq. (2) yields a curve falling below the data for times shorter than about 100 μs and at times longer than 500 μs . The fitting curve lies somewhat above the data at intermediate times. A distinctly better fit is obtained by scaling the initial intensity by $\exp(0.1)$ to avoid the initial exponential decay not envisioned in the derivation of Eq. (2). A similar, but more subtle, pattern exists in the data for 4% Nd. The energy transfer parameters obtained from fitting the data at each concentration are given in Table 1. Comparison with the data for 532-nm excitation shows that the single-step transfer to randomly-spaced acceptors appears stronger under 808-nm excitation than under 532-nm excitation, whereas the migration transfer rate shows the opposite trend.

As Fig. 2(a) shows, a straightforward fit of the 9% Nd sample's fluorescence decay waveform also lies below the data at short times. It is necessary to scale the initial intensity by $\exp(0.07)$ to obtain a satisfactory fit to this waveform. Since there is no evidence of an initial exponential decay in any of the other high-concentration decay waveforms obtained in

this study, this is surprising. However, close inspection of the data shows that it is only the first data point in the 9% Nd, 808-nm-excited data that deviates significantly from Eq. (2). Also, the 9% signal actually falls less rapidly for the first few data points than does the 8% signal, not to be expected due to the higher concentration and the faster subsequent decay. The most plausible explanation is that the first data point in the 9% trace occurred before the rollover of the laser pulse was complete, resulting in an offset in the time scale of the 9% data set.

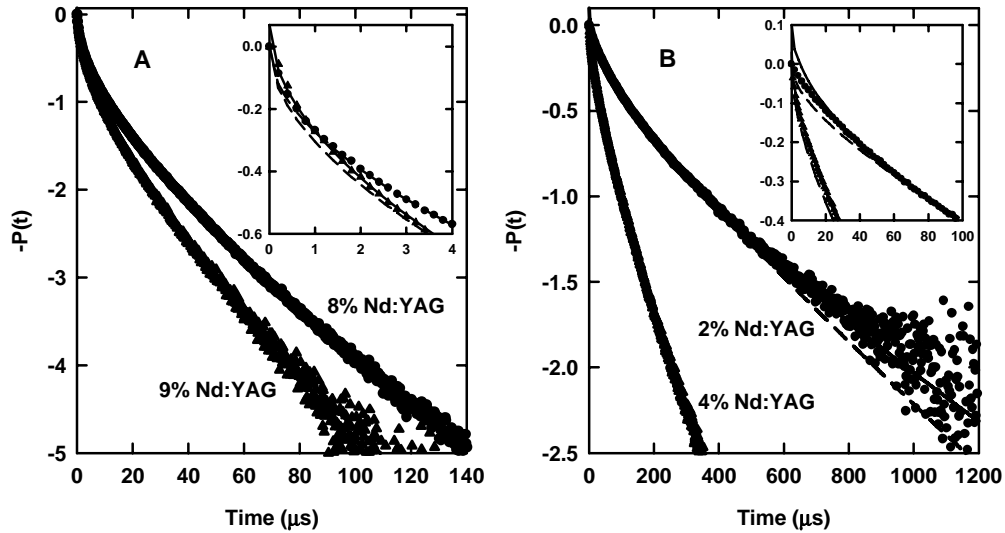


Fig. 2. Quenching function $P(t)$, as defined by Eq. (1) with $\tau_0 = 262 \mu\text{s}$, for the short-pulse, 808-nm excited fluorescence of bulk samples of ceramic Nd:YAG for four concentrations, with the insets showing the early-time behavior. In each case the discrete symbols represent the experimental data. Fits to Eq. (2) are shown as solid and dashed curves. For 2, 4 and 9% Nd the fit shown as a solid curve has its amplitude scaled to fit the portion of the decay after the initial approximately exponential decay, whereas the fit shown as a dashed curve is an attempt to fit the entire decay at once.

Table 2. Comparison of fluorescence decay kinetics under 808-nm excitation by long pulses (several μs) and by short pulses (several ns).

Nd Concentration (% atomic)	τ (long-pulse) (μs)	$t_{1\text{st e-fold}}$ (short-pulse) (μs)	τ_{tail} (short-pulse) (μs)
0.09	252	262	262
1	224	232	260.5
2	170	158	218
4	96	75	125
8	28	12	59
9	31	9	52

Since Kumar *et al.* report exponential decays following 807-nm excitation using chopped CW diode light for excitation, it is possible that our very different results are related to pulse duration. To test this possibility we measured the fluorescence decays of the same samples used in the preceding sections, using 808-nm pulses several milliseconds in duration. These pulses were provided by chopping the output of a CW Ti:sapphire laser such that the cut-off time was less than two microseconds. The duty factor was 50%. We observed single exponential decays for all Nd concentrations, to within experimental error. The lifetimes are given in Table 2, together with the lifetimes that best fit the exponential tails and first e-

folding times of the decays observed under short-pulse excitation at the same wavelength. The long-pulse-excited lifetime values are consistent with those of Kumar *et al.*, up through the 4% maximum concentration reported in that study [5]. These values are generally intermediate between the initial e-folding times and tail lifetimes observed under short-pulse excitation.

6. Discussion

6.1. Concentration dependence of energy transfer

The concentration dependences of the energy transfer fitting parameters obtained from Eq. (2) and the short-pulse experiments of the preceding sections are shown in Fig. 3. Although quantitative details differ among the three sets of experiments, patterns are evident. The concentration dependences of the energy migration inferred from the tail lifetimes and the single-step transfer inferred from the earlier \sqrt{t} behavior of the quenching function are clearly different, and will be discussed separately.

As Figs. 3(a), 3(c), and 3(e) show, the energy migration quenching rate increases quadratically with Nd concentration. Yokota and Tanimoto's treatment of diffusion-limited energy transfer showed that the transfer rate in the migration regime (hence at long times after the excitation pulse) is proportional to the acceptor concentration and to the diffusion constant (describing migration among donor ions) to the three-quarters power [10]. Standard treatments of diffusion among the donors show that the diffusion constant is proportional to the inverse fourth power of the average spacing between neighboring donors, and hence is directly proportional to the four-thirds power of the donor concentration [12]. Thus, the transfer rate in the migration regime is directly proportional to the donor concentration and to the acceptor concentration. By the nature of transfer by energy migration, in which donors are sufficiently common for many donor-donor transfer steps to occur before a donor-acceptor step, the donor concentration is at least approximately proportional to the total Nd concentration and is likely to be nearly equal to it. Thus, the observed quadratic dependence indicates that the acceptor concentration is also proportional to the total Nd concentration. In the Yokota-Tanimoto model the linear dependence on acceptor concentration reflects the probability that an excited donor is near enough to an acceptor for donor-acceptor transfer to occur before further donor-donor migration. In the present case, if the positions of the Nd ions are uncorrelated, the probability that an excited ion has another Nd ion sufficiently nearby to cross-relax rapidly (before fluorescing and before any further migration) is proportional to the Nd concentration. Thus, the linear relationship between acceptor concentration and Nd concentration is consistent with quenching by cross-relaxation.

Note from Fig. 3 that the exponential tail quenching rate for the 1% sample falls below the quadratic functions that best fit the higher concentration data in all three experimental conditions. This may indicate that the average Nd ion spacing at that low concentration is too large for the same diffusion-like kinetics to describe this case. However, since the tail lifetimes of the 0.09% and 1% samples are similar, the inferred migration quenching rate for 1% Nd is quite sensitive to small errors in extracting the lifetimes. This limits the physical significance of the deviation at 1%.

The magnitude of the migration transfer rate versus concentration may be obtained by fitting the curves of Fig. 3 to a line with the slope fixed at 2.0, and averaging the resulting y-intercepts. The result, $W([\text{Nd}]) = [\text{Nd}]^2 \times 245 \text{ s}^{-1} (\% \text{ atomic})^{-2}$, is in excellent agreement with the $[\text{Nd}]^2 \times 240 \text{ s}^{-1} (\% \text{ atomic})^{-2}$ reported by Lupei *et al.* for energy migration in Japan Fine Ceramics Center material [2]. Thus, there is no reason to suspect different energy migration kinetics for ceramics from these two sources, which use significantly different formation processes [1, 13].

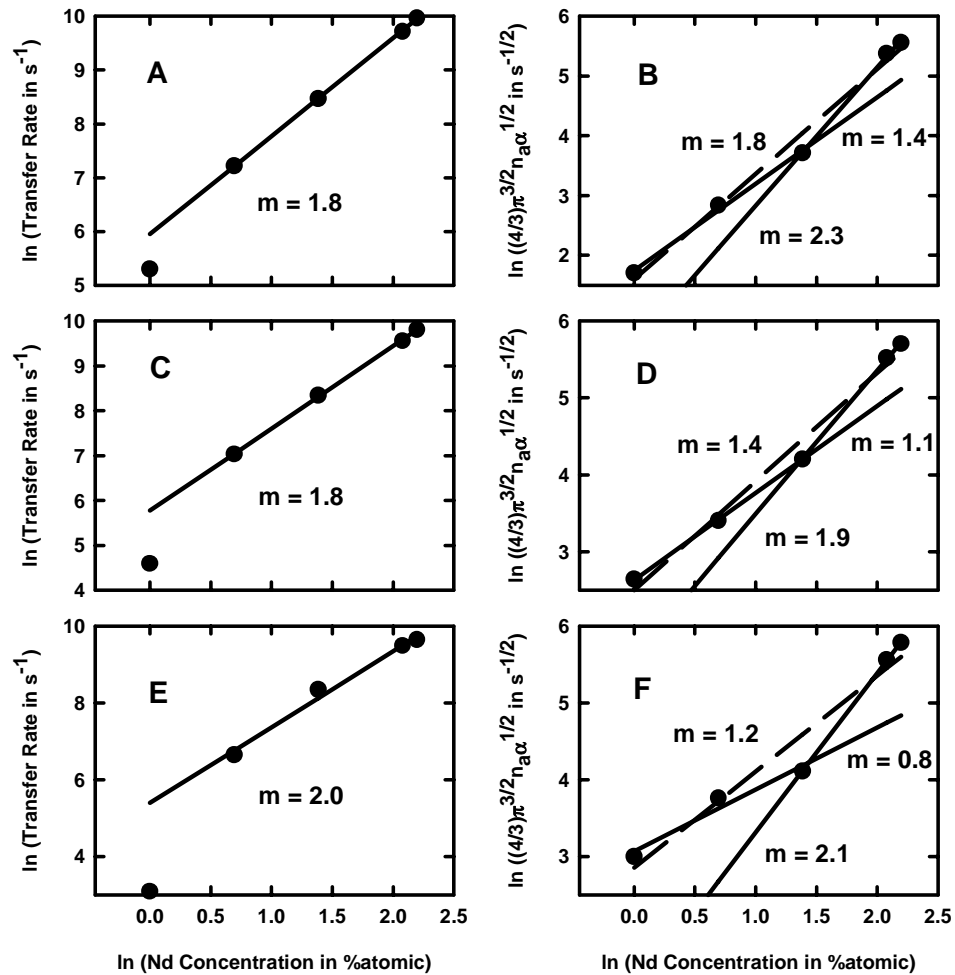


Fig. 3. Concentration dependence of the energy transfer parameters for short-pulse-excited fluorescence of ceramic Nd:YAG. Filled circles are the fitting parameter values from Table I; solid lines are linear regression fits. A and B are the results for 532-nm excitation of bulk samples, C and D are for 532-nm excitation of powder samples, and E and F are for 808-nm excitation of bulk samples.

For single-step transfer the observed concentration dependence is rather more complex. Since the ordinate in Fig. 3(b), 3(d) and 3(f) depends on the concentration of acceptors, the power-law dependence of this quantity on Nd concentration should straightforwardly indicate whether the acceptors are related to single Nd ions or to pairs. Yet, fits to the full range of concentrations give slopes averaging about 1.5, consistent with neither of these models. The key to interpreting the results lies in the fact that the quantity $(4/3)\pi^{3/2}n_a(\alpha)^{1/2}$ for a concentration of 4% lies below the best fit to the full concentration range in all three data sets. Indeed, it appears that the slope is lower for the concentrations 1-4% and higher for 4-9%. Fig's. 3(b), 3(d) and 3(f) also show fits to these concentration subsets. The slopes average

about one for the lower concentrations and about two for the higher concentrations, suggesting that in the single-step regime transfer to isolated Nd ions dominates at low concentrations and transfer to pairs becomes more important above 4% Nd.

6.2. Relationship to low-concentration studies

V. Lupei and A. Lupei developed their model for single-crystal Nd:YAG, in which data were only available for relatively low concentrations. They assumed transfer by direct cross-relaxation between excited ions and unexcited ions at random distances, and since this makes practically every Nd ion an acceptor, this model predicts a linear dependence of the transfer rate on Nd concentration [6]. For their single-crystal Nd:YAG data, with its limited range of concentrations, this model fit the data quite satisfactorily. It may be similarly adequate to the single-step transfer observed for low concentrations in the present study. However, the quadratic dependence observed in the present study for single-step transfer at higher concentrations is clearly inconsistent with this direct cross-relaxation model. Instead, our results favor the model of resonant transfer to cross-relaxing Nd pairs. It should be noted that the quadratic concentration dependence of energy transfer by migration, observed both by us and by Lupei [2], does not provide similar help in determining whether random-range or near-neighbor cross-relaxation better characterizes quenching of the acceptors involved in that process. This is so because in either case, the probability of a given donor having neighbors sufficiently close to quench rapidly is proportional to the total Nd concentration.

Lupei and Lupei argued that their model required a much smaller (and more physically plausible) value for the electric-dipole-dipole interaction parameter, α , than does resonant migration to Nd pairs. Indeed, their α , $1.85 \times 10^{40} \text{ cm}^6 \text{ s}^{-1}$, is smaller than that of Ref. 7 by a factor of 60-80. Which of these values is more plausible? Rough estimates of the expected α value can be made from the classic Forster-Dexter model.

Following the approach of Danielmeyer [14], and assuming for simplicity that for each given set of overlapping emission and absorption lines the widths of the absorption and emission lines are equal, one can express the interaction parameter as follows.

$$\alpha(d \rightarrow a, \text{EDD}) \cong (27c^4/64\pi^6 n^3 v_{da}^4 \tau_{d0}) \sum_i \beta_i \sigma_{ai}(\text{pk}) / (1 + (v_{di} - v_{ai})^2 / \Delta v_i^2) \quad (3)$$

Here n is the refractive index, v_{da} is the average photon frequency of the overlapping donor emission and acceptor absorption transitions, τ_{d0} is the radiative lifetime of the donor ion, the sum is over all pairs, i , of donor emission and acceptor absorption lines with significant spectral overlap, β_i is the emission line branching ratio for the i^{th} line pair, $\sigma_{ai}(\text{pk})$ is the peak cross section of the absorption transition involved in the i^{th} pair, v_{di} and v_{ai} are the photon frequencies of the i^{th} donor emission peak and acceptor absorption peak, and Δv_i is the full width at half maximum of the donor and acceptor lines in the i^{th} pair. The frequencies, linewidths, branching ratios and absorption cross sections for the cross-relaxation process, (${}^4\text{F}_{3/2}$, ${}^4\text{I}_{9/2} \rightarrow {}^4\text{I}_{15/2}$, ${}^4\text{I}_{15/2}$), are taken from Ref. 14, except that the absorption strengths have been scaled to our absorption data by the ratio of our 1743 nm absorption cross section to their slightly different value. The resulting value of the interaction parameter is:

$$\alpha(\text{cross-relaxation, Forster-Dexter}) \approx 6.4 \times 10^{40} \text{ cm}^6 \text{ s}^{-1}. \quad (4)$$

For resonant transfer, (${}^4\text{F}_{3/2}$, ${}^4\text{I}_{9/2} \rightarrow {}^4\text{I}_{9/2}$, ${}^4\text{F}_{3/2}$), Eq. (3) is simplified by the fact that for each overlapping pair of lines $v_{di} = v_{ai}$. The emission branching ratios are available from standard monographs [15], and we observe the effective absorption cross sections to be (in units of 10^{-21} cm^2) 21, 5.5, 2.7, 10, 9, 4.4 and 1.5 for the peaks at 869, 875, 879, 884, 885, 890 and 900 nm, respectively. The resulting value of the interaction parameter is:

$$\alpha(\text{resonant transfer, Forster-Dexter}) \approx 3.3 \times 10^{38} \text{ cm}^6 \text{ s}^{-1}. \quad (5)$$

These α values are each about 2-3.5 times the values reported by Lupei . and Diaz-Torres . for their energy transfer models [2, 7]. Given the approximations involved, such as approximate linewidths and the neglect of inhomogeneity, such agreement is not unreasonable. The large difference between α (cross-relaxation) and α (resonant transfer) is due about equally to the weaker emission and the weaker absorption involved in cross-relaxation. The ratio α (resonant transfer)/ α (cross-relaxation) has a similar value for the theoretical α 's, 52, to that for the models of Refs. [2] and [7]. Thus the quite different parameter values required to fit energy transfer data by the models in those references are, in fact, both physically plausible. This makes it entirely possible that both processes play a role or even that direct cross-relaxation dominates at low concentrations with the other mechanism becoming dominant as the concentration increases. Our observed transition from approximately linear concentration dependence of the single-step transfer at low concentrations to approximately quadratic dependence at higher concentrations provides evidence that this is, in fact, the case.

6.3. Complex behavior under 808-nm excitation

The well-established rapid, efficient nonradiative decay from ${}^4G_{7/2}$ through the intervening levels to the metastable ${}^4F_{3/2}$ leads one to expect the same decay kinetics regardless of which manifold within that range is excited. Thus, it is reassuring that our results give roughly similar decay waveforms for 532-nm and 808-nm excitation by short pulses. This strongly suggests that the striking difference between the decay kinetics reported in Refs. [2], [4], and [5] is not due to excitation wavelength. We do observe just such a difference when we compare short-pulse and long-pulse excitation of the same set of samples at 808 nm, indicating that the difference in materials among Refs. [2], [4] and [5] is also not decisive. Also, since variation of pump intensity at 532 nm yielded no evidence of changed kinetics in our experiments, neither nonlinear processes nor changes in quenching due to differences in heating are likely to explain the difference.

Rather, the difference in observed decay waveforms between Q-switched and chopped CW excitation is most plausibly due to details being masked by the lower-intensity, long-pulse chopped CW excitation. When excited by a pulse longer than the fluorescence lifetime, the signal adds the contributions only over a portion of the pump pulse comparable to that lifetime. Recall also that, for all but the lowest concentrations used in this study, short-pulse excitation showed a distinctly slower decay of the exponential tail relative to the initial decay rate. It follows that under long-pulse excitation the slow tail signal can sum contributions over a considerably larger portion of the excitation pulse than can the fast initial decay. This makes the fast initial decay less prominent in the signal under long-pulse excitation than under short-pulse excitation. In addition, the chopped CW excitation source has lower peak intensity, so that the dynamic range between the maximum signal and the noise floor is smaller—typically less than two e-foldings for the chopped CW results reported here versus about five e-foldings using the Q-switched pump sources. The limited dynamic range in the chopped CW case makes it more difficult to discern deviations from exponential decay. Thus, it is probable that the nominally single exponential decays reported here and in Ref. [5] are artifacts of the excitation format. It may be noted from Table 2 that the lifetimes measured under long-pulse excitation tend to be intermediate between the fast initial and exponential tail lifetimes from the short-pulse excited waveforms, particularly for concentrations sufficiently high that the initial and tail lifetimes differ substantially. This suggests that the long-pulse experiments capture some average decay rate, consistent with the above interpretation.

6.4. Variations with excitation wavelength

Although the decay curves under short-pulse excitation are similar for the three sets of data, there are quantitative differences. In the case of the powdered samples, the differences may perhaps be attributed to the poorer signal to noise ratio that results from much shorter

absorption paths, but the differences in decay kinetics of bulk samples excited at 532 nm compared to 808 nm are more likely to be meaningful.

The absorption data presented in Fig. 4 provide a clue to the difference in behavior with pump wavelength. This figure shows the effective ground state absorption cross section (that is, absorption coefficient divided by total Nd concentration,) versus wavelength over intervals including the two pump wavelengths for three of the Nd concentrations used in this study. The data are for a 1% Nd:YAG sample whose measured Nd concentration is $1.39 \times 10^{20} \text{ cm}^{-3}$, a 4% sample and a 9% sample. Spectra were repeated with slightly different slit widths and for different sampling intervals, and were found to be reproducible. Comparison indicates that as the Nd concentration increases some peak positions and linewidths change perceptibly. This indicates a degree of inhomogeneous broadening, even at room temperature, and must be due to changes in the crystal field as Nd ions come to have more Nd ions as near neighbors.

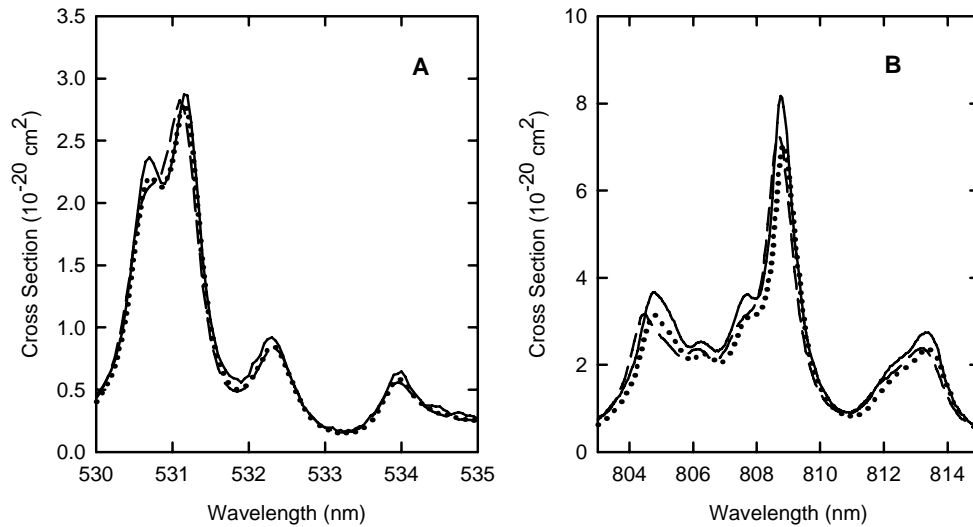


Fig. 4. Effective ground state absorption cross section of ceramic Nd:YAG near 532 nm and 808 nm for different concentrations. Solid curves: 1% Nd; dotted curves: 4% Nd; dashed curves: 9% Nd.

These absorption spectra suggest that the model of Eq. (2) is too simple. Since the absorption data indicate that Nd ions with Nd neighbors at different distances and in different numbers have somewhat different spectra, their transition strengths and thus their electric-dipole-dipole interaction strength parameters may well also vary among different donors. This results in two effects. Firstly, no model that assumes a single rate parameter for the single-step transfer and a single diffusion rate constant is likely to fit the decay kinetics precisely. Secondly, the variations in spectra for different concentrations suggest that we may have performed inadvertent site-selection experiments, with the degree of selectivity varying with concentration and with excitation wavelength. Thus, the somewhat different decay kinetics observed at the different excitation wavelengths could be due to excitation of different subsets of Nd ions.

6.5. Approximately exponential decay at early times

We observe an approximately exponential initial decay, similar to that reported by Lupei . [6, 11], but only at relatively low Nd concentrations (consistently for 1% and 2%, and in one experiment for 4%.) The very plausible interpretation offered by Lupei *et al.* for this initial

decay provides a basis for explanation of this concentration dependence. The model that results in Eq. (2) assumes a uniform distribution of acceptors right up to zero spacing. The finite minimum spacing between donor and acceptor ions in any real system establishes a finite maximum energy transfer rate, and thus prevents the decay from becoming faster without limit for times approaching the moment of initial excitation. One would need detailed knowledge of the acceptor distribution around each donor to predict the exact deviation from Eq. (2) on the basis of this model. However, even in the absence of such detail, it is clear that the distance from a typical donor to its nearest acceptor must tend to decrease as the acceptor concentration increases. Thus, the time period during which Eq. (2) is valid will extend closer to the time of initial excitation for high concentrations than for low. Since we chose the sampling parameters for our experiments to cover several e-foldings, the time resolution is not sufficient to follow the kinetics at very early times, and thus it is not surprising that we observe the effect only at modest concentrations.

7. Conclusions

In conclusion, we have studied the fluorescence decay of Konoshima fine-grained ceramic Nd:YAG for Nd concentrations from 0.09 to 9 % atomic at two different excitation wavelengths. The quadratic concentration dependence of the migration transfer rate inferred from the exponential tail of the decay curve is consistent with quenching by cross relaxation between Nd ions, but does not make clear whether the quenching occurs primarily within closely-spaced pairs, or whether pairs at many spacings contribute substantially. The nonexponential decay observed at earlier times agrees satisfactorily with the familiar model of single-step transfer to acceptors at random distances from a donor. The complex concentration dependence of the rate parameter for this transfer is best explained by assuming that transfer to two-ion quenching centers dominates at high concentrations, but that direct cross-relaxation between isolated ions dominates for concentrations below about 4%. Theoretical estimates of energy transfer rate parameters for both processes indicate that the two are competitive, so that such a cross-over at intermediate concentrations is plausible.

The observation of somewhat different decay rates at two different excitation wavelengths and the differences in absorption spectra at different concentrations both point to the likely importance of spectral inhomogeneity. Given the variation with concentration and the high quality of the ceramics under study at low concentration, this inhomogeneity is almost certainly due to the random distribution of dopant ions. This suggests that, although satisfactory optical properties have been reported for ceramic Nd:YAG up to the several percent dopant level, the material quality is in fact reduced at high Nd concentrations, at least in regard to its spectroscopic properties. This inhomogeneity may also be responsible for the higher passive losses inferred from laser experiments on high-concentration ceramic Nd:YAG [16]. It would be worthwhile for site-selection spectroscopy to be performed on these materials, not only at low temperatures where inhomogeneities have been detected in many materials, but also at room temperature.

One practical result of this study is that one clearly must expect a fast initial decay prior to the exponential tail in the decay of highly-doped ceramic Nd:YAG, regardless of excitation wavelength or source of the ceramic. This results in reduced energy storage time, on average, and thus will limit the efficiency of highly-doped Nd:YAG for lasers unless the pump pulse is kept short compared to the first e-folding times displayed in Table 2 [16]. This is a more demanding constraint than would be inferred from the longer tail lifetimes or those observed under long-pulse excitation. Since high Nd concentration may well be desirable in other respects, such as to increase pump absorption in samples thin enough for efficient cooling, this nonexponential decay must be taken into account when selecting the optimum concentration and pumping method.

Acknowledgments

The authors wish to thank Prof. Daryush ILA and his students at the Alabama A&M University Research Institute for Nd concentration measurements, and Dr. Gregory Quarles and colleagues at VLOC, Inc. for preparing the samples investigated in this work. This work was funded in part by the High Energy Lasers Joint Technology Office. Work of S. M. H. was supported by the Air Force Contract No. F33615-00-C-5422